Circulation

RESEARCH LETTER

PTPMT1 Is Required for Embryonic Cardiac Cardiolipin Biosynthesis to Regulate Mitochondrial Morphogenesis and Heart Development

Ze'e Chen, PhD; Siting Zhu, BS; Hong Wang, MS; Li Wang, BS; Jianlin Zhang, PhD; Yusu Gu, MD; Changming Tan, MD; Mehul Dhanani, BS; Eric Wever, MS; Xinru Wang, BS; Boyu Xie, BS; Shijia Wang, MD; Lei Huang, MD; Antoine H.C. van Kampen, PhD; Jie Liu, PhD; Zhen Han, MD; Hemal H. Patel, PhD; Frédéric M. Vaz, PhD; Xi Fang, PhD; Ju Chen, PhD; Kunfu Ouyang, PhD

Cardiolipin is a unique glycerol-bridged dimeric phospholipid representing up to 20% of total lipids in mitochondrial membranes in cardiomyocytes. Abnormal cardiolipin metabolism is linked to heart diseases, including Barth syndrome, myocardial ischemia-reperfusion injury, and heart failure.[1] However, cardiolipin profiles and specific roles of cardiolipin in cardiac mitochondria remain largely obscure.

We first performed quantitative lipidomic analysis on mouse hearts at different stages and revealed a strong discrepancy in molecular compositions of cardiolipin and cardiolipin-related metabolites between embryonic and adult mouse hearts (Figure [A]). In particular, cardiolipin in embryonic hearts displayed more diverse acyl compositions, while the predominant form of cardiolipin in the adult heart was tetralinoleoyl cardiolipin, implicating that the pathways involved in cardiolipin biosynthesis and metabolism may have different functions between embryonic and adult hearts.

To investigate the role of cardiolipin biosynthesis in cardiac development, we used cardiac Troponin T (*TnT-Cre*) to generate a mouse model with cardiac-specific deletion of PTPMT1 ([protein tyrosine phosphatase mitochondrial 1] CKO), a mitochondrial phosphatase that removes the terminal phosphate group from phosphatidylglycerophosphate to form phosphatidylglycerol,[2] to disrupt cardiolipin biosynthesis in embryonic hearts. PTPMT1 deficiency indeed reduced the contents of both total cardiolipin and most of the abundantly expressed cardiolipin species in embryonic hearts at both embryonic day 11.5 (E11.5) and embryonic day 15.5, accompanied with a broad alteration in levels of total and individual cardiolipin-related metabolites (Figure [B and C]), demonstrating that PTPMT1 is required for cardiolipin biosynthesis in embryonic cardiomyocytes. All mouse protocols were approved by the Institutional Animal Care and Use Committee.

Deletion of PTPMT1 in cardiomyocytes caused abnormal cardiac development and embryonic lethality between embryonic day 16.5 and embryonic day 18.5. Morphological changes started in CKO hearts at embryonic day 12.5 (Figure [D]), accompanied with decreased thicknesses of ventricular walls at the same stage (Figure [E and F]), which could be a consequence of defects in cardiac cell proliferation first observed in compact zone of CKO hearts at E11.5 (Figure [G and H]).

Cardiolipin has been proposed to participate in regulating both mitochondrial function and structure.[1] We then evaluated mitochondrial respiration in permeabilized embryonic hearts by measuring oxygen consumption. Decreases in respiratory function of complex I and maximum oxidative phosphorylation capacity were observed in CKO hearts as early as E11.5 (Figure [I]). At embryonic day 12.5, respiratory functions were further impaired, and changes in expression of mitochondrial complex proteins were observed in CKO hearts (Figure [I and J]).

In developing embryonic cardiomyocytes, mitochondria undergo a maturation process with increased mitochondria number and more organized lamellar cristae

Key Words: cardiolipins ■ mitochondria ■ mitochondrial membranes ■ myocytes, cardiac ■ protein tyrosine phosphatases

Correspondence to: Ju Chen, PhD, or Xi Fang, PhD, Department of Medicine, University of California San Diego, 9500 Gilman Drive, La Jolla, CA, 92093; or Kunfu Ouyang, PhD, School of Chemical Biology and Biotechnology, State Key Laboratory of Chemical Oncogenomics, Peking University Shenzhen Graduate School, Shenzhen 518055, China. Email juchen@health.ucsd.edu or xifang@health.ucsd.edu or ouyang_kunfu@pku.edu.cn

For Sources of Funding and Disclosures, see page 404.

Circulation is available at www.ahajournals.org/journal/circ

Nonstandard Abbreviations and Acronyms

CKO	TnT-Cre-mediated cardiac-specific PTPMT1 knockout
E11.5	embryonic day 11.5
MICOS	mitochondrial contact site and cristae organizing system
PTPMT1	protein tyrosine phosphatase mitochondrial 1

at later stages.[3] The function of cardiolipin in regulating mitochondrial morphology and ultrastructure in embryonic hearts remains unclear. We performed transmission electron microscopy analysis, and found that membrane invagination was impaired and a bubble-like inner membrane structure—instead of lamellar cristae—could be easily observed in CKO mitochondria at E11.5, and became more severe at embryonic day 12.5 (Figure [K]). PTPMT1 deletion also altered mitochondrial diameter, percentages of mitochondria with lamellar cristae, cristae lengths, and cristae numbers in embryonic cardiomyocytes (Figure [L–O]), suggesting that PTPMT1-mediated cardiolipin biosynthesis is required for normal mitochondrial morphogenesis and cristae biogenesis in developing cardiomyocytes. Because cristae are recognized as fundamental structures to provide a sufficient area and proper spatial organization for oxidative phosphorylation and other membrane proteins in mitochondria,[4] abnormalities in cristae biogenesis could account for dysfunctional mitochondrial respiration in E11.5 CKO hearts.

The F1F0-ATP synthase dimers, MICOS (mitochondrial contact site and cristae organizing system) complex, OPA1 (optic atrophy protein 1 mitochondrial dynamin-like guanosine triphosphatase), and prohibitin proteins, have been proposed to participate in regulating mitochondrial cristae biogenesis.[5] ATP5I (ATP synthase, H+ transporting, mitochondrial F0 complex, subunit E) and ATP5L (ATP synthase, H+ transporting, mitochondrial F0 complex, subunit G), 2 components of F1F0-ATP synthase, were downregulated in CKO hearts at E11.5. The dimerization of F1F0-ATP synthase complex was also impaired, while the assembly of complex monomer remained unaffected in CKO hearts at the same stage (Figure [P and Q]). It is interesting that deletion of PTPMT1 in cardiomyocytes impaired the assembly of MICOS complex in CKO hearts at E11.5 but did not alter the expressions of individual MICOS components (Figure [R and S]). Furthermore, we did not observe significant differences in the expressions of MFN1 (mitofusin 1), MFN2 (mitofusin 2), OPA1 (optic atrophy 1 mitochondrial dynamin-like guanosine triphosphatase), DRP1 (dynamin-related protein 1), FIS1 (mitochondrial fission 1 protein), and prohibitin proteins between control and CKO hearts at E11.5 (Figure [T]).

We also generated an inducible cardiac-specific *Ptpmt1* knockout mouse model using α*MHC-CreER*. Induced deletion of PTPMT1 in adult mouse cardiomyocytes by tamoxifen reduced phosphatidylglycerol (34:1), the most abundant phosphatidylglycerol species, and increased phosphatidylglycerophosphate (34:1), the most abundant phosphatidylglycerophosphate species (Figure [A and C]), indicating that PTPMT1 is also responsible for catalyzing the conversion from phosphatidylglycerophosphate to phosphatidylglycerol in adult hearts. Although PTPMT1 deficiency also altered the levels of monolysocardiolipin and dilysocardiolipin (Figure [B and C]), the levels of total cardiolipin and individual cardiolipin species remained intriguingly unchanged (Figure [B and C]), and no morphological and functional changes were observed in the cardiomyocytes of adult mice with induced deletion of PTPMT1 (Figure [U–W]).

Taken together, our results demonstrated an essential role of PTPMT1-mediated cardiolipin biosynthesis in regulating mitochondrial cristae morphogenesis in embryonic mouse cardiomyocytes and heart development. Our results also revealed a difference in not only the composition but also the metabolism of cardiolipin and cardiolipin-related metabolites between embryonic and adult hearts.

ARTICLE INFORMATION

The data, analytical methods, and study materials that support the findings of this study will be available to other researchers from the corresponding authors on reasonable request.

Affiliations

Department of Cardiovascular Surgery, Peking University Shenzhen Hospital, School of Chemical Biology and Biotechnology, State Key Laboratory of Chemical Oncogenomics, Peking University Shenzhen Graduate School, Shenzhen, China (Z.C., S.Z., H.W., X.W., B.X., S.W., L.H., Z.H., K.O.). Departments of Medicine (Z.C., S.Z., L.W., J.Z., Y.G., C.T., X.F., J.C.); and Anesthesiology (M.D., H.H.P.), School of Medicine, University of California San Diego, La Jolla. Department of Cardiothoracic Surgery, The Second Xiangya Hospital, Central South University, Changsha, Hunan, China (C.T.). Department of Pathophysiology, School of Medicine, Shenzhen University, Shenzhen, China (J.L.). Veterans Administration San Diego Healthcare System, CA (M.D., H.H.P.). Departments of Clinical Chemistry and Pediatrics, Amsterdam Gastroenterology Endocrinology Metabolism (E.W., F.M.V.); and Core Facility Metabolomics (E.W., F.M.V.), Laboratory Genetic Metabolic Diseases; Bioinformatics Laboratory, Department of Epidemiology and Data Science, Amsterdam Public Health Research Institute (E.W., A.H.C.v.K.), Amsterdam Universitair Medische Centra; and Biosystems Data Analysis, Swammerdam Institute for Life Sciences (A.H.C.v.K.), University of Amsterdam, The Netherlands.

Sources of Funding

Drs J. Chen, Fang, and Patel are funded by grants from the National Heart, Lung, and Blood Institute of the US National Institutes of Health. Dr J. Chen holds an American Heart Association Endowed Chair in Cardiovascular Research. This work was also supported by the National Science Foundation of China (81970421 to K.O.), the Shenzhen Basic Research Foundation (JCYJ20190808174001746 to K.O.), the Shenzhen-Hong Kong Institute of Brain Science-Shenzhen Fundamental Research Institutions (2019SHIBS0004), the National Institutes of Health (HL091071 to H.H.P.), and the Veterans Administration (BX001963 and BX005229 to H.H.P.).

Disclosures

Dr J. Chen has consulted for and receives research funding from MyoKardia Inc.

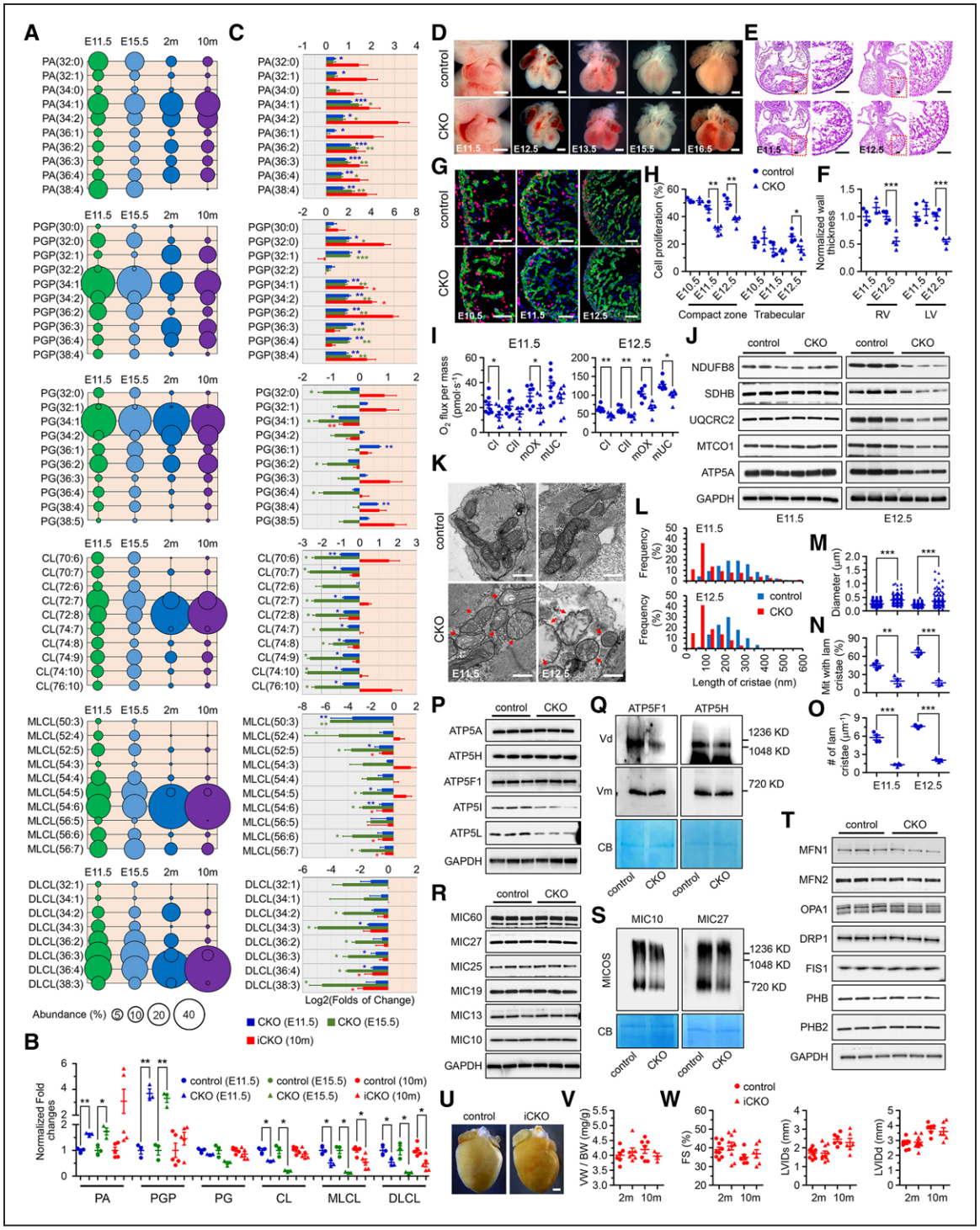

Figure. PTPMT1 is required for embryonic cardiac cardiolipin biosynthesis to regulate mitochondrial morphogenesis and heart development.

A, Quantitative lipidomic analysis was applied to identify individual species of cardiolipin and cardiolipin-related metabolites, including PA, PGP, PG, CL, MLCL, and DLCL in the ventricles of control mice at E11.5, E15.5, 2 months, and 10 months of age, respectively. All the species of each metabolite, or the 10 most abundant species if more than 10 species were observed, were selected and further analyzed at each stage. The abundance (%) of individual species was calculated according to its total level and is represented by the area of the circle (n = 3, 3, 6, and 6, respectively). **B**, The levels of total PA, PGP, PG, CL, MLCL, and DLCL in CKO ventricles at E11.5 (n = 3) and E15.5 (n = 3), and in iCKO ventricles 10 months post–tamoxifen-induced gene deletion (n = 5) were analyzed and normalized to their control ventricles (n = 3, 3, and 5, respectively). Twenty-five and 6 ventricles with the same genotype were pooled as 1 sample at E11.5 and E15.5, respectively. **C,** The levels of every species, or the levels of the 10 most abundant species if more than 10 species were observed, of PA, PGP, PG, CL, MLCL, and DLCL in CKO and iCKO ventricles were further analyzed and normalized to their control ventricles, respectively. **D** through **H,** Representative images of embryonic hearts **(D)**, sections stained with hematoxylin and eosin **(E)**, and images of EdU labeling (*Continued*)

Figure Continued. (**G**) of control and CKO mice at indicated stages. Cardiac cells were costained with α-actinin. Scale bar = 0.5 mm, 100 μm, and 50 μm, respectively. The thickness of left and right ventricular walls (**F**) of control (n = 4 at both stages) and CKO (n = 3 and 4, respectively) hearts, and the ratios of EdU-positive cardiomyocytes in ventricular compaction zone and trabecular (**H**) of control (n = 3, 4, and 4, respectively) and CKO (n = 3, 5, and 5, respectively) hearts were measured at indicated stages. **I,** Oxygen flux representing the respiratory function of CI and CII, mOX, and mUC were measured in control and CKO hearts by high-resolution respirometry at E11.5 and E12.5, respectively. The measurement was performed on 2 hearts with the same phenotype at E11.5 or 1 heart at E12.5 in one chamber (n = 8 per group at E11.5; n = 6 per group at E12.5). (**J**) Immunoblot analysis on the expression of mitochondrial oxidative phosphorylation subunits including NDUFB8 (complex I), SDHB (complex II), UQCRC2 (complex III), MTCO1 (complex IV), and ATP5A (complex V) in control and CKO embryonic hearts at E11.5 and E12.5. GAPDH was used as the loading control. **K,** Representative transmission electron microscopic images of mitochondria in control and CKO cardiomyocytes at E11.5 and E12.5. Red arrows indicate the mitochondria with bubble-like cristae in CKO cardiomyocytes. Scale bar = 0.5 μm. **L** through **O,** Quantitative analysis of length of cristae (**L**), mitochondrial diameter in the short axis (**M**), the percentage of mitochondria with lamellar cristae (**N**), and the number of lamellar cristae along the mitochondrial long axis (**O**) in control and CKO cardiomyocytes at E11.5 (n = 4 per group) and E12.5 (n = 3 per group). At least 160 mitochondria were measured for each embryonic heart. **P** through **T,** Immunoblot analysis of F1F0-ATP synthase subunits (**P**) including ATP5A, ATP5H, ATP5F1, ATP5I, and ATP5L, MICOS complex subunits (**R**) including MIC60, MIC27, MIC25, MIC19, MIC13, and MIC10, as well as mitochondrial dynamics–related proteins (**T**) including MFN1, MFN2, OPA1, DRP1, and FIS1 and prohibitin proteins including PHB and PHB2 at E11.5. GAPDH was used as the loading control. Blue Native-PAGE and immunoblot analysis of F1F0-ATP synthase complex using the antibodies against ATP5F1 and ATP5H (**Q**), and MICOS complex assembly using the antibodies against MIC10 and MIC27 (**S**). To note, the deletion of PTPMT1 reduced the formation of F1F0-ATP synthase dimers, whereas monomers were not affected. The reduction of the MICOS complex assembly in CKO mitochondria was also observed. Each mitochondrial sample was prepared from more than 50 embryonic ventricular tissues of the same genotype in 1% digitonin-containing extraction buffer, and separated by Blue Native-PAGE. CB-stained membranes were scanned for loading control. **U**, Representative hearts of control and iCKO mice at 10 months post–tamoxifen injection. Scale bar = 1 mm. **V**, Ratios of ventricle weight to body weight in control and iCKO mice at 2 months and 10 months post–tamoxifen injection (n = 3 to 7 mice per group). **W**, Echocardiographic assessment in control and iCKO mice at 2 months and 10 months post–tamoxifen injection (n = 6 to 10 mice per group). All data represent mean±SEM. Significance was determined by 2-tailed, unpaired Student *t* test. **P*<0.05, ***P*<0.01, ****P*<0.001 vs control. ATP5A indicates F1 complex subunit α; ATP5F1, F0 complex subunit b; ATP5H, F0 complex subunit d; ATP5I, F0 complex subunit e; ATP5L F0 complex subunit g; CB, Coomassie blue; CI, complex I; CII, complex II; CKO, *TnT-Cre*-mediated cardiac-specific PTPMT1 knockout; CL, cardiolipin; DLCL, dilysocardiolipin; DRP1, dynamin-related protein 1; E11.5, embryonic day 11.5; E12.5, embryonic day 12.5; E15.5, embryonic day 15.5; FS, fractional shortening; GAPDH, glyceraldehyde 3-phosphate dehydrogenase; iCKO, αMHC-Cre^{ER}–mediated PTPMT1 knockout; KD, kilodaltons; LV, left ventricle; LVIDd, left ventricular internal diameter end diastole; LVIDs, left ventricular internal diameter end systole; mOX, maximum oxidative phosphorylation capacity; mUC, maximum uncoupled capacity; MLCL, monolysocardiolipin; MTCO1, mitochondrially encoded cytochrome C oxidase I; MICOS, mitochondrial contact site and cristae organizing system; MIC60, MICOS complex subunit Mic60; MIC27, MICOS complex subunit Mic27; MFN1, mitofusin 1; MFN2, mitofusin 2; NDUFB8, 1,4-dihydronicotinamide adenine dinucleotide:ubiquinone oxidoreductase subunit B8; OPA1, optic atrophy protein 1 mitochondrial dynamin-like guanosine triphosphatase; PA, phosphatidic acid; PG, phosphatidylglycerol; PGP, phosphatidylglycerophosphate; PHB, prohibitin; PHB2, prohibitin 2; PTPMT1, protein tyrosine phosphatase mitochondrial 1; RV, right ventricle; SDHB, succinate dehydrogenase [ubiquinone] iron-sulfur subunit B; UQCRC2, cytochrome b-c1 complex subunit 2, mitochondrial; Vd, F1F0-ATP synthase dimer; Vm, F1F0-ATP synthase monomer; and VW/BW, ventricle weight/body weight.

REFERNCES

1. Dudek J, Hartmann M, Rehling P. The role of mitochondrial cardiolipin in heart function and its implication in cardiac disease. *Biochim Biophys Acta Mol Basis Dis*. 2019;1865:810–821. doi: 10.1016/j.bbadis.2018.08.025
2. Zhang J, Guan Z, Murphy AN, Wiley SE, Perkins GA, Worby CA, Engel JL, Heacock P, Nguyen OK, Wang JH, et al. Mitochondrial phosphatase PTPMT1 is essential for cardiolipin biosynthesis. *Cell Metab*. 2011;13:690–700. doi: 10.1016/j.cmet.2011.04.007
3. Dorn GW II, Vega RB, Kelly DP. Mitochondrial biogenesis and dynamics in the developing and diseased heart. *Genes Dev*. 2015;29:1981–1991. doi: 10.1101/gad.269894.115
4. Cogliati S, Frezza C, Soriano ME, Varanita T, Quintana-Cabrera R, Corrado M, Cipolat S, Costa V, Casarin A, Gomes LC, et al. Mitochondrial cristae shape determines respiratory chain supercomplexes assembly and respiratory efficiency. *Cell*. 2013;155:160–171. doi: 10.1016/j.cell.2013.08.032
5. Pfanner N, Warscheid B, Wiedemann N. Mitochondrial proteins: from biogenesis to functional networks. *Nat Rev Mol Cell Biol*. 2019;20:267–284. doi: 10.1038/s41580-018-0092-0